A New Approach Combining a Multilayer Radiative Transfer Model with an Individual Based Forest Model: Application to Boreal Forests in Finland

Hans Henniger [1,2,*] , **Friedrich J. Bohn** [1] , **Kim Schmidt** [1,3] **and Andreas Huth** [1,2,4]

1   Helmholtz Centre of Environmental Research - UFZ; Permoserstr. 15, 04318 Leipzig; hans.henniger@ufz.de, friedrich.bohn@ufz.de, andreas.huth@ufz.de

2   Institute for Environmental Systems Research, University of Osnabrück, Barbara Straße 12, 49074 Osnabrück, Germany

3   Remote Sensing Centre for Earth System Research, Talstr. 35, 04103 Leipzig; kim.schmidt@ufz.de

4   iDiv German Centre for Integrative Biodiversity Research Halle-Jena-Leipzig, Puschstraße 4, 04103 Leipzig, Germany

*   Correspondence: hans.henniger@ufz.de

Abstract: To understand forest dynamics under today's changing environmental conditions, it is important to analyze the state of forests at large scales. Forest inventories are not available for all regions, so it is important to use other additional methods, e.g. remote sensing observations. Increasingly, remotely sensed data based on optical instruments and airborne LIDAR are becoming widely available for forests. There is great potential in analyzing these measurements and gaining an understanding of forests states. In this work, we combine the new generation radiative transfer model mScope with the individual-based forest model FORMIND to generate reflectance spectra for forests. Combining the two models allows us to account for species diversity at different height layers in the forest. We compare the generated reflectances for forest stands in Finland, in the region of North Karelia, with Sentinel-2 measurements. We investigate which level of forest representation gives the best results and explore the influence of different calculation methods of mean leaf parameters. For the majority of the forest stands, we generated good reflectances with all levels forest representation compared to the measured reflectance. Good correlations were also found for the vegetation indices (especially NDVI with $R^2 = 0.62$). This work provides a forward modelling approach for relating forest reflectance to forest characteristics. With this tool it is possible to analyze a large set of forest stands with corresponding reflectances. This opens the possibility to understand how reflectance is related to succession and different forest conditions.

Keywords: forest model; radiative transfer; vegetation indices; individual based; forest reflectance

1. Introduction

Forest play a major role in the terrestrial component of the global carbon cycle. They account for about 55% of global aboveground carbon stock [1] and represent approximately 40% of the global terrestrial carbon sink [2,3]. Forests shape the surface of the Earth by comprising 31% of the land area [4] and they influence the energy balance by reflecting and absorbing sunlight. They are important for sustaining biodiversity and provide habitat for 70% of all faunal species [5–7]. Forests exhibit a diversity of spatial structures that can be dynamic due to natural succession, management or disturbances [8].

To monitor the state of forests, the conventional standard practice for foresters and ecologists alike has long been measurement of forest inventories. Collecting inventories is time consuming. However, in tropical forests, national forest inventories are often missing. Another approach to monitor forests is based on remote sensing observations which provide relevant data at large scales. The amount of data is significantly raising with more and more earth observing satellite missions that were launched in the last ten years [9]. The spatial and temporal remote sensing observations offer the opportunity to get a better understanding of forests with respect to their structure and dynamics.

Satellite measurements vary in their resolution and coverage. Thus, for global observations, there is a trade-off between the spatial and temporal resolution of satellite (e.g., Landsat, Sentinel) and airborne products. The combined methods of remote sensing and field observations offers the opportunity to get a better understanding of forests with respect to their structure and dynamics. However, the ecological interpretation of remote sensing observations of forests is challenging, and in many cases still in development.

One way to obtain information from remote sensing measurements concerning target vegetation variables (e.g. Leaf Area Index (LAI), species composition, productivity), is to use models that link the measured remote sensing measurements to the vegetation. Vegetation models have been successfully applied to study change in forests for nearly four decades, many of which differ in their applications. One example, dynamic global vegetation models (e.g. ED by [10] and CLM4 by [11]) were initially developed to represent the interaction between vegetation and the global carbon cycle as stand-alone simulation models, but also to represent vegetation dynamics in the context of Earth System Models, or alongside atmospheric (General Circulation Models), oceanic, and the cryospheric modeling frameworks [12]. These models focus on large scale applications and they rely on simplifications to reduce complexity and computational demand (e.g. individual species simplified to plant functional types). They do not offer information at the individual tree level. For the analysis of forests in forestry and ecology, there is a long tradition [13] of using individual forest models (e.g. FORMIND by [14] and LPJ-GUESS by [15]). FORMIND is able to represent the ecosystem dynamics of the forest by simulating each individual tree in a forest (forest gap model). FORMIND allows the simulation of species rich forests and also considers the size and age structure of the simulated tree community. At the same time, with increasing computing capacity, there is an opportunity to use these models to simulate large forest areas. Due to the simulation of single trees, they are also able to consider the heterogeneity of forest structure and dynamics.

An important component in vegetation models is solar irradiance and the competition for light between plants. One simple way to calculate the light climate is based on Lambert-Beer's law, which is often used by forest models. It describes the decreasing intensity of radiation as it passes through a medium (e.g. tree crowns), depending on the composition of the medium and the height of the layer. Radiative transfer models (RTMs) calculate the light climate in the forests in a more detailed way. They simulate the reflectance, interception, absorption, and transmission of light through a canopy. Radiative transfer is influenced e.g. by the amount of leaves, their characteristics (i.a. amount of chlorophyll and carotenoids, water content), the angle of leaves at which light strikes the leaf, and the angle between leaves and the sun. All these parameters are combined by coupled differential equations and allow the calculation of reflectance of a forest for light of different wavelengths (between 300 nm to 2500 nm - depending on the model) including reflectance, absorption and transmission of the leaves. Some RTMs are able to provide results for multiple canopy layers, whereas others assume a homogeneous canopy. RTMs are able to simulate the reflectance of the canopy, as it is measured by satellites. Canopy radiative transfer is one of the primary and long relied upon mechanisms by which models relate vegetation properties to surface reflectance as captured by remote sensing [16] radiative transfer in combination with vegetation can be modelled in different levels of complexity. The representation of the vegetation for which the radiative transfer is calculated can range from a simple homogeneous to a detailed and heterogeneous 3D representation of the vegetation structure. The complexity of the solution of radiative transfer problems also varies [17,18] from numerical Monte Carlo ray tracing approaches (e.g. [19,20]) to analytical solutions using e.g. four stream technology (e.g. [21]).

Some of the global vegetation models are coupled with simple RTMs to calculate reflectance for wavelength from 300 to 2500 nm. The two-stream approximation is used to calculate radiative transfer in CLM4.5 [22], ED2 [23] and CLM(SPA) [24]. Mostly these models use only a few plant functional types and a low number of canopy layers.

With the new generation of RTMs (like DART by [25] and mScope by [26]) it is possible to consider heterogeneous vegetation. The more complex the structure of the vegetation is, the more computationally intensive the simulation of light reflectance and the interaction with the vegetation. The same applies to the simulation of vegetation on a global level. As mentioned, global vegetation models must make strong simplifications in order to be able to simulate large areas in appropriate timespans. Individual-based models describe forest structure in a more detailed way, but they are difficult to apply on a global scale because of the computational requirements. Nevertheless, they endorse the fundamental premise that the structure of forests represents an important factor for ecosystem dynamics that is lost in more aggregated modelling approaches [13].

Individual based forest models in combination with the new generation of RTMs are therefore a promising approach to consider the complexity of forest structure and species. Their combination will aid in the development of a mechanistic understanding of the linkage between forest reflectance and forest properties like structure and species diversity. The challenge is to develop an approach which is sensitive to forest structure and species diversity within the current, but ever-increasing computational constraints both in simulating vegetation and radiative transfer, in order to allow the analysis of huge forest simulations. Such a tool can be also used to get a more general understanding of the relationships between reflectance and vegetation properties.

Here, we present an approach by coupling the new generation RTM mScope with the individual-based forest model FORMIND. We enlarge the application field of mScope and investigate the calculated reflectance spectra of boreal forests using forests in Finland as an example. Comparing the simulation output with Sentinel-2 data allows us to answer the following questions: How does the concept of forest representation (homogeneous or heterogeneous structure) influence the reflectance spectrum? Can the approach reproduce the variety of reflectance spectra in Finland? And how well can we calculate the vegetation indices of the forests with this approach?

2. Materials and Methods

For coupling the individual-based forest model FORMIND and the radiative transfer model RTM mScope, we implemented mScope (in an adapted version of [26]) as an additional process in the forest model FORMIND. By using inventories for forest stands in Finland and the forest model, we are able to reconstruct these forests. In combination with the RTM it is possible to calculate reflectance spectra for the visible and near infrared range. We then compare the simulated reflectance with measured reflectance spectra from remote sensing observations (Sentinel-2).

To analyze possible applications, different levels of the forest complexity were analyzed and their influence on the reflection spectra was investigated. In addition, several vegetation indices were calculated and analyzed.

2.1. Study site

For this study we investigated 28 boreal forest stands in Finland in the region of North Karelia, which are located in an area of about 150 km × 150 km (see Figure A1). The inventory data was collected for the FunDivEUROPE project (http://www.fundiveurope.eu) [27] in summer (August) in 2012 and again in 2017. Each of the 28 inventory plots has a size of 30 m × 30 m (Figure 1). The forest inventory contains information on species type, tree positions (x- and y-coordinates) and stem diameters at breast height from all trees. Information about the understory (e.g. shrubs, grasses, mosses) are not provided by the inventory. Based on stem diameter and tree species, other important forest attributes, such as tree height, crown diameter, Leaf Area Index (LAI) are calculated by the forest model FORMIND. The investigated forest stands include as main species Picea Abies (Norway spruce), Pinus Sylvestris (Baltic pine), Betula Pendula (silver birch), and Betula Pubescens (downy birch). Information about species richness and evenness, biomass, basal area and LAI can be found in Table A2 and Table A5.
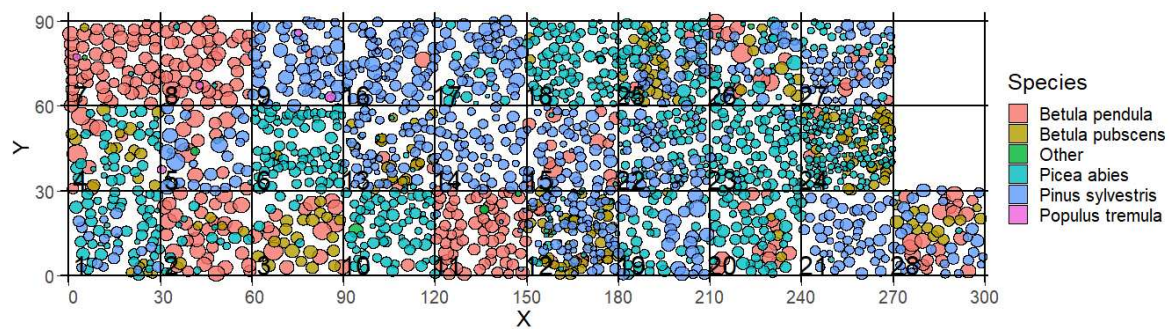
Figure 1. Visualisation of the forest inventory of the 28 forest stands in Finland (reconstruction of 2015). Each circle represents a tree and its location in the plot (x and y coordinates). The color of the circles represents the species of a tree and the size of the circle represents its crown diameter. The number in the squares indicates the number of the forest stand and corresponds to the numbering in the FORMIND simulation. The forest stands are shown the side by side but are originally distributed over an area of 150 km × 150 km (a map is shown in Appendix Figure A1).

For all forest stands tree size were measured in 2012 and 2017. Here we took the mean stem diameter (at breast height) of the measured stem diameter values of 2012 and 2017, as a proxy for the stem diameter in the year 2015 (same year as the analysis of Sentinel-2 data [28]) and used these values for the forest reconstruction with FORMIND. We then compared the calculated reflectance spectra with remote sensing observation using atmosphere-corrected Sentinel-2 measurements [28] from July respectively August 2015. For the simulation of the reflectance spectra, information on observation geometries (sun and observer, in terms of zenith and azimuth) for each forest stand were provided by [28].

2.2. The individual-based forest model FORMIND

For the simulation of the 28 forest stands we used the individual- and process-based forest model FORMIND, which belongs to the model family of individual-based forest gap models. This means that the growth of every single tree is simulated and that individual trees interact with each other. Additionally, FORMIND allows the simulation of forests with different tree species and also considers the size structure of the tree community. FORMIND can be used for small scale simulations as well as large scale simulations [29,30] e.g. in the Amazon.

The model includes four main process groups: recruitment, mortality, competition (e.g. for light and space), and growth of each individual tree (increment of tree biomass, stem diameter and height). For our investigations, we have implemented the RTM mScope as an additional process in FORMIND (in an adapted version in C++).

The stem position (x- and y-coordinate), species information and the diameter at breast height is used as input information in FORMIND. Via different allometry formulas, FORMIND calculates tree height, crown diameter, and LAI. This also depends on a set of species-specific parameters and allometry equations. FORMIND has been extensively tested and applied to tropical forests [30–38], temperate forests [39–41], grasslands [42] and boreal forests [43]. The parameterization of [39] includes all tree species of the investigated forest stands (North Karelia, Finland) and is used for our simulations on a 30 m × 30 m scale.

2.3. Coupling mScope with FORMIND

MScope is an RTM which on the one hand can handle several canopy layers and on the other hand has a short computation time. For this study we [26] coupled mScope with FORMIND (as a part of the FORMIND code). It is based on Scope (Soil Canopy Observation of Photochemistry and Energy fluxes, [44]). The Scope model is a vertical one dimensional, integrated radiative transfer and energy balance model, which simulates short wave reflectance spectra (400 – 2500 nm) and the fluorescence

of homogeneous vegetation. In its original version, it combines two basic RTMs: Fluspect [45] (on the base of PROSPECT, [46]) for calculations of reflectance, transmittance, and fluorescence at leaf level and SAIL based models (Scattering by Arbitrary Inclined Leaves, Verhoef [47]) for calculating the radiative transfer in the canopy. Compared to Scope, mScope has multiple layers to include variation in the distribution of leaves which enable the representation and simulation of heterogeneous vegetation.

We use mScope [26] to simulate the reflectance spectra of forest stands. For calculations at leaf level (reflectance, transmittance, and fluorescence), our mScope version uses the model PROSPECT-D [46]. At canopy level (radiative transfer), a modified version of Scope is used.

For the parameterization of the leaf model following attributes are used:

- leaf structure (number of internal leaf layers [layer])
- the amount of pigments in the leaf (chlorophyll a and b [μg cm^{-2}], carotenoids [μg cm^{-2}], anthocyanins [μg cm^{-2}], senescent pigments [fraction])
- dry matter [g cm^{-2}] and leaf water content [g cm^{-2}]
- traits describing vegetation structure as the mean and bi-modality of the leaf inclination distribution function, LAI [m^2 m^{-2}], canopy height [m]

The parameters for the different species were taken from the "CABO 2018-2019 Leaf-Level Spectra Data set" by [48] and can be found in Table A1. These values are generalized values (measurements from Finland were not available). Due to physiological similarities, species Betula Pendula and Betula Pubescens are combined to one species group called Betula (birches). Additional information that are used are soil reflectance spectra (see Figure A2) and atmospheric constants, which are taken from [26].

2.4. Representations of different levels of forest complexity (heterogeneous structure)

Using the individual-based approach in forest modeling, it is possible to simulate and describe forest structure at fine scales, which allows for the heterogeneity of a forest to be considered. Individual-based forest models (here FORMIND) make it possible to gain tree- and forest-specific properties for each forest patch (e.g. 30 m × 30 m) in different height layers (each height layer has a thickness/size Δh) from the bottom/soil up to the top of the canopy.

One important property to calculate radiative transfer is the LAI. FORMIND enables the calculation of LAI distributions for each tree over height (the above described height layers). In order to determine the species composition, we used the LAI fraction of a species as a measure of its abundance. MScope uses a fixed number of height layers (in the version of [28]: 60 layers). In our modified version we use a fixed layer height $\Delta h = 10$ m for a low height resolution and later $\Delta h = 0.5$ m for a high resolution (see Figure A4). We analyse forests up to forest heights of 50 m. Thus, we use 5 or 100 height layers, respectively, for our calculations. Depending on the structure of the forest, leaves are located in different height layers. Height layers without leaves do not contribute to the reflectance spectra.

To calculate leaf reflectance and transmittance (using the leaf model PROSPECT-D), the RTM utilized information from the forest model for each layer, which included a leaf parameterization containing leaf properties for each layer. Additionally, the distribution of the orientation of leaves was considered – it was assumed to be spherical for all species, but it is also possible to choose other distributions. MScope also includes observation geometry (sun and satellite, azimuth and zenith). Vegetation information from the reconstructed simulated forest, which is delivered by the forest model was able to be processed in different ways and then be transferred to the radiative transfer model. In this paper, we analyze three cases, for which each consequence to a different representation of the vegetation. The processing differs according to the LAI and according to the species composition (Figure 2).
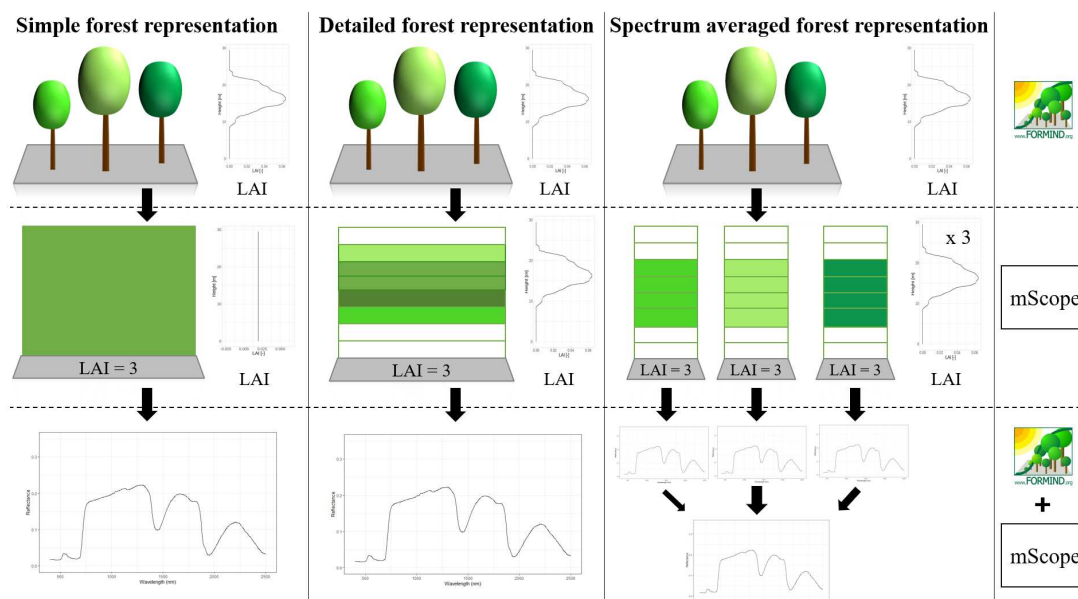
Figure 2. Different concepts of forest representation Visualization of the different representations of a sample forest during the simulation (1st column: Simple forest representation, 2nd column: detailed forest representation, 3rd column: spectra-averaged forest representation). We see how, under the given concept, the forest is represented in FORMIND (1st row), how it is simulated in mScope (2nd row) and how the output is built (3rd row). The sample forest has 3 different species (represented by the different colours). The concepts of representation are described in detail in the text.

1. Simple forest representation

   The simplified forest representation, uses only reduced information of the forest. It assumes the same mixture of species and the same LAI for each height layer of the forest stand. The leaf parameterization is calculated by averaging the leaf attributes of the occurring species (weighted by LAI, as a measure of abundance). The LAI of the forest stand is equally distributed among all layers.

2. Detailed forest representation

   The detailed representation of the forest, assigns to each height layer different mixtures of species and different LAIs. The leaf parameterization for each layer is calculated by averaging the leaf attributes of the occurring species weighted by LAI in the height layer, as a measure of abundance. For each layer of the forest, the calculated LAI of the reconstructed forest stand will be used.

3. Spectra-averaged representation

   In this case, the forest is divided into different "sub-forests". In each sub-forest stand, we maintain the total number of trees and the structure of the main forest stand. However, we assume that all trees in a sub-forest stand are of only one species. Thus, there are as many sub-forests as there are tree species. For each layer, the calculated LAI of the reconstructed forest stand is used. For each of these single-species sub-forests, the reflectance spectra are calculated using the species-specific leaf parameters. Final reflectance spectrum is determined by averaging the species-specific spectra weighted by LAI fraction, as a measure of abundance.

The processed Sentinel-2 observations [28] include reflectance values for only 10 wavebands. MScope calculates radiative transfer for wavelengths in the range of 400 nm to 2500 nm (with a resolution of 1 nm). For better comparability with the simulated reflectance profiles, we averaged the simulated reflectance values for the different Sentinel-2A bands (e.g. Sentinel Band 704 nm has a range of 15 nm, so we averaged 15 reflectance values; more information on bands see Appendix Table A3). This averaged values are shown as dots in Figure 3, 4 and A13 and are the basis of the comparisons with Sentinel-2 measurements.

Vegetation indices derived from canopy reflectance are widely used in remote sensing, as they represent proxies for vegetation attributes (e.g. LAI, productivity). We calculated several vegetation indices (NDVI, EVI, MSI, in appendix: NDMI, kNDVI). NDVI is chlorophyll sensitive. EVI [49] is responsive to canopy structural variations, including LAI, canopy type and plant physiognomy [50]. We also analyzed kNDVI [51] as a modification of the NDVI. The NDMI is partly correlated with the water content of the canopy [52]. [53] introduced the moisture stress index (MSI, [54]), which utilises reflectance wavebands in the SWIR (1550 - 1750 nm) and NIRS (760 - 900 nm). Additional to the vegetation indices we analyzed the similarity index SAD [55] (spectral angle distance see Appendix Figure A12 and Table A4).

In the mScope model, some code adjustments were made to account for the structure of the forest models and forests from the inventory. In forests models it is possible that there are layers without leaves (vertical gaps). The adjustments were necessary to ensure that these layers had no influence on the reflectance spectrum. MScope calculates the probability of viewing a leaf in solar (P_S) and observer direction (P_O) by assuming a homogeneously distributed LAI in the forest.

$$P_S = e^{k \cdot xl \cdot LAI} \tag{1}$$

$$P_O = e^{K \cdot xl \cdot LAI} \tag{2}$$

with xl as negative cumulative layer thickness, k as extinction coefficient in direction of sun, LAI as Leaf Area Index of forest stand and K as extinction coefficient in direction of sun.

This leads to the situation that the probability is also influenced by layers with a LAI of 0. We have changed the calculation equivalently allowing different LAI values for the height layers.

$$P_S = e^{-k \cdot LAI(i)} \tag{3}$$

$$P_O = e^{-K \cdot LAI(i)} \tag{4}$$

with $LAI(i)$ as Leaf Area Index in height layer i of forest stand, k as extinction coefficient in direction of sun and with K as extinction coefficient in direction of sun.

The mScope code also includes a correction of P_S and P_O, which we also considered.

3. Results

First, to reduce the complexity of the analysis, we analyzed the reflectance of even-aged forests, where the RTM uses a low resolution (height layer size Δh = 10 m, Figure 3). In each layer a homogeneous leaf distribution is assumed. The even-aged forest stands number 17, which was dominated by one species and stand number 5 which contained three species were used as examples for this analysis. Reflectance was then calculated for simplified, detailed and spectra-averaged forest representations.

There were differences (up to 140%) in reflectance between the detailed (blue) and the simplified (orange) forest representation. The simplified representation consistently produced higher reflectance (especially in comparison to spectra-averaged representation). Both the modelling and satellite measurements show different reflectance spectra for the two forests. We found a higher similarity of reflectance for the detailed representation.

In the next part of the investigation, we increased the represented complexity of the forest. This was done by assuming a layer height of 0.5 m (Figure 4). Here, the forest model (here FORMIND) provided mScope with a higher resolution distribution of LAI and species-specific information over height. As in Figure 3, results are again shown for the simplified, detailed and the spectra-averaged representation of the forests for both example sites.
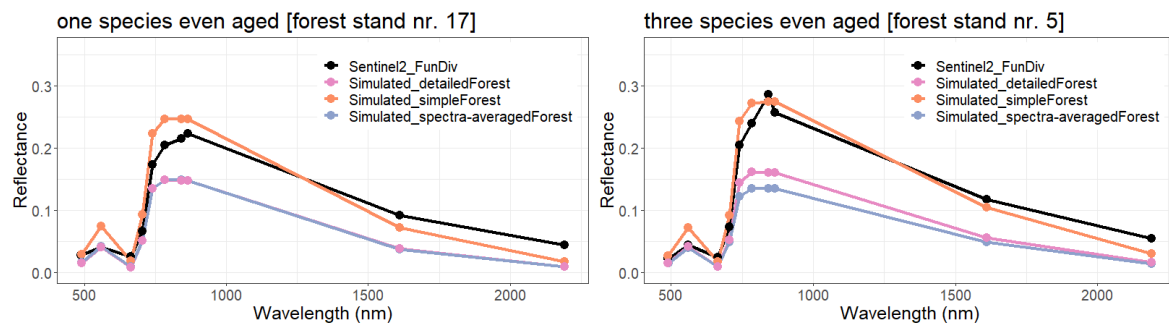
Figure 3. Reflectance spectra for detailed and simplified forest representation by using layers of 10 m height. Visualization of the calculated reflectance profiles for two forest stands (number 5 and 17) in Finland. Forest stand number 17 (left - mainly one species) and forest stand number 5 (right - three species). Both forest stands are even-aged (small standard deviation of tree heights: 4.6 m and 4.5 m). Each point represents the reflectance value averaged over the specific bands (corresponding to the bands of Sentinel-2). Sentinel measurements are shown in black and simulated reflectance is shown in orange/blue/pink from coupling a forest model (FORMIND) with mScope. We used 10 m height layers. The reflection of all other forest stands is shown in the Appendix (Figure A6).
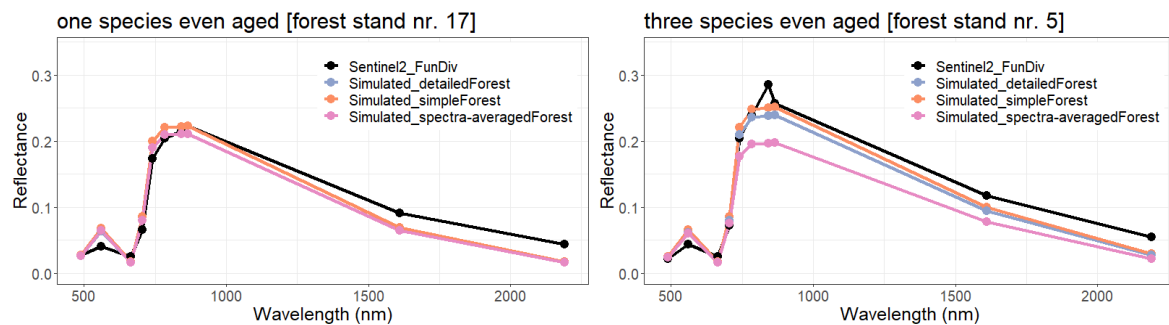
Figure 4. Reflectance spectra for detailed and simplified forest representation by using standard layers of 0.5 m height. Visualization of the calculated reflectance profiles for two forest stands (number 5 and 17) in Finland according to Figure 2 is shown. Each point represents the averaged reflectance value over the specific bands (corresponding to the bands of Sentinel-2). Sentinel measurements are shown in black and simulated reflectance is shown in orange/blue/pink from coupling a forest model (FORMIND) with mScope. We use here 0.5 m height layers. The reflection of all other forest stands is shown in the Appendix (Figure A10) Additionally, the reflection for the complete spectra of all other forest stands is shown in the Appendix (Figure A11). Additionally we calculated the spectral angle distance for all comparisons (see Appendix Figure A12).

All three versions produced comparable reflectance spectra (especially for forest stand number 17). The lowest reflectances were produced with the spectra-averaged forest representation (in particular for forest stand number 5 with underestimating the NIR values). For forest stand 17 the spectra-averaged forest representation produces the same reflectance values as the detailed forest representation version. As the forest stand contains only one species, there is no averaging in the leaf parameters and spectra, and we got the same results for these versions. Results for all bands were in agreement with the Sentinel measurements.

The simulated reflectance spectra also enabled the calculation of vegetation indices (see section 2.3). We analyzed NDVI, EVI and MSI (kNDVI and NDMI in appendix Figure A19) for each forest stand and for each forest representation (Figure 5). Each were then compared with indices calculated using the satellite observations.
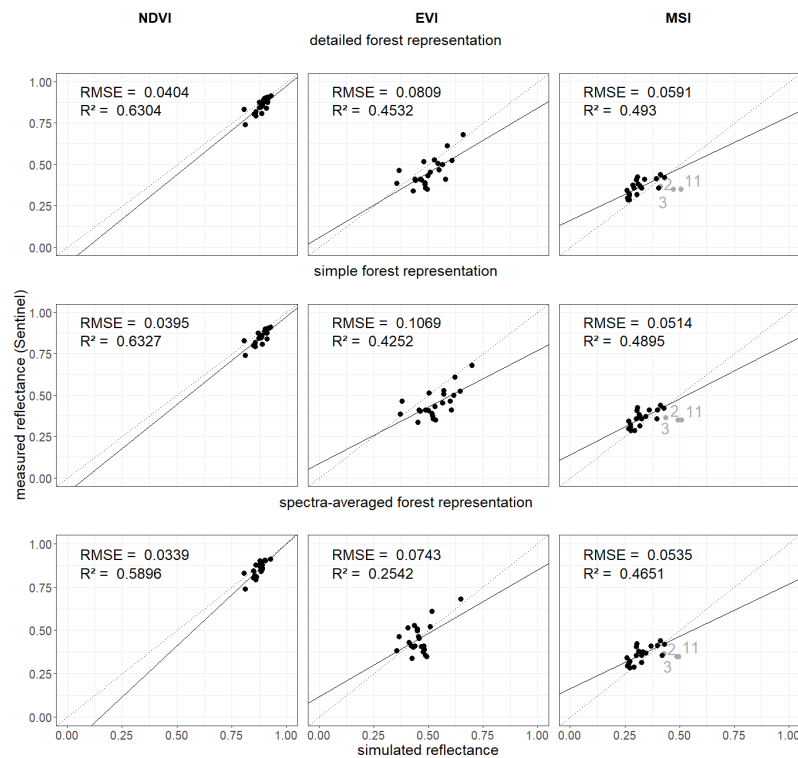
Figure 5. Comparison of vegetation indices. The vegetation indices (NDVI left, EVI middle, MSI right) are calculated from the reflectance values in the different wavebands once for the simulated reflectance spectra and for the satellite measurements. In each row, a different forest representation is used to calculate the results of the indices from the simulated spectra (1. detailed forest representation, 2. simple forest representation, 3. spectra-averaged forest representation; more information about the cases in section 2.3). Each point represents a forest stand in Finland (gray points indicate birch forest stands that are not used to calculate the RMSE and R^2 - see Appendix Figure A14 - A17). Results for the calculation of the NDMI and the kNDVI can be found in the Appendix (Figure A19). We excluded five forest stands from our analysis due to inconsistencies in Sentinel-2 measurements (see Appendix Figure A14 - A17).

We obtained different results for all 3 forest representations when analyzing NDVI, EVI, and MSI. Lower R^2 and higher RMSE values are obtained for MSI. Measured Sentinel-2 values were close to each other. NDVI values from simulated reflectance spectra were within small ranges. We found an R^2 of 0.63 (detailed forest representation) when comparing simulated and measured NDVI values. For the EVI, there is a larger range of values. EVI led to a lower R^2 (about 0.45) and higher RMSE (0.08) for compared to NDVI. The MSI of birch forest stands were overestimated (gray points). Detailed and simple forest representation show similar results for all three indices.

4. Discussion

In this work, we developed a new approach to study forest reflectance for radiation in the visible and near infrared spectrum. For this, we coupled the individual-based forest model FORMIND with an adapted version of the radiative transfer model mScope. We then used the coupled models to reconstruct 28 forest stands in Finland and calculate reflectance spectra for each. We analyzed three different concepts of forest representation: simple, detailed and spectra-averaged.

When we compare the simulated reflectance spectra with the Sentinel measurements, the best results where achieved for the detailed forest representation. However, measured reflectance of forests stands with similar forest structure and species mixture show large differences in five cases (Appendix Figure A14 - A17). Analysis of these cases (outliers) suggests that factors other than LAI distribution and species composition are here responsible for the differences such as limitations in the atmospheric

correction or overlapping of tree crowns in the neighborhood of the forest stands. In addition to that the approach show potential of improvement in the sensitivity of simulated reflectance for Sentinel-2 bands B01, B03 and B04. The quality of the simulated reflectance spectrum does not depend on certain species or forest structures (we did not find general relations). This study provides a baseline for further research. The coupling of individual based forest models and multi-layer RTMs opens the opportunity to analyse a vast range of forests with various structure and species mixtures and to gain a deeper understanding of reflectance spectra of complex forests (e.g. influence of tree allometries, leaf parameters or role of understory).

An important aspect of our study is the representation of the forest in the the RTM. The simple and detailed forest representations use an averaged leaf parameterization for each height layer (using the LAI of the occurring species as weighting factor). In the spectrum-averaged version, we simulate each occurring species as a monoculture forest and afterwards average the resulting reflectance spectra (using the LAI of the occurring species as weighting factor). Despite the non-linear nature of the RTM, the best results are obtained when the input leaf parameters are averaged (simple and detailed concept). Less good results are obtained when the output reflectance (reflectance spectra for each species) is averaged (spectra-averaged concept). We obtained similar results for simple and detailed forest representation. The NDVI values were all within a smaller range. As only a few of the analyzed stands have a LAI below 2.5, we observed also a saturation of the NDVI values [56]. Forest stands covering a broader spectrum of LAI values will allow to a more general comparison of satellite-based and modelled indices and should be conducted in future studies. For the EVI values lower correlation and a higher RMSE compared to the NDVI analysis was observed.

A challenge for the parameterization of radiative transfer models is the selection of suitable parameters (e. g. for leaf attributes, soil and leaf angle distribution). There are a large number of measurements available that include different leaf parameters. However, the leaf parameters of each species can vary depending on the site, the position of the leaf within the canopy, the day of the year of the measurement and environmental factors [57]. Therefore, leaf parameterizations from sites with the most comparable environmental conditions should be used. A sensitivity analysis [58–61] was used to analyze the influence of leaf parameters on the reflectance spectrum. In particular, higher sensitivity [48] is observed for those parameters that influence the visible light spectrum (e.g. pigments). Using hyperspectral data, this approach can also be used to fit species parameters.

For soil reflectance, often a wet soil type is assumed (due to lack of data) and in this study, we followed this approach. Nevertheless, it would also be possible to model the soil reflectance spectrum with an additional model (e.g.BSM model by [62]).

In this study we developed a forward modelling tool for connecting forest reflection with forest properties. There are further interesting analyses possible based on this approach. One example would be to analyze more complex forests, such as tropical forests. The information about reflectance can be used as an addition to e.g. LIDAR measurements to analyze forest structure and functions. It is useful to point out here that the forest model is not only able to investigate structural information but is also able to calculate characteristics of forest dynamics such as productivity. The combination of height dependent information about forest structure with the information about light reflection spectra might give sufficient information about structure and species composition, resulting in the capability to derive e.g. estimates of current carbon pools. In addition to the work by [63], the presented approach allows to improve the matching of satellite measurements (e.g. LIDAR profiles) to forest simulations considering spatially heterogeneous environmental and ecological conditions. As a result, it can improve the carbon estimates for large regions. Please note that the presented approach could be used to derive simulated LIDAR profiles (and thus may improve the LIDAR model used in the mentioned study).

Importantly, this approach can also be used to generate a large number of reflectance spectra for forests by simulating forests over time and tracking reflectance spectra. This would allow us to understand the dynamics of reflectance spectra during forest succession. Disturbed forests show

similar characteristics as forests in early and mid-successional phase. We can use this knowledge to characterize disturbed forests based on reflectance. This my help us to distinguish better between natural and disturbed forests.

However, forest simulations also include path dependencies. Not all types of forest might be covered in simulations which might occur due to management or disturbances. To overcome this, the Forest Factory approach [64,65] generates a broad range of forest states covering various types of forest structures and species compositions. This approach can also be used to figure out which forests or forest states provide the same reflectance spectrum opening up the possibility of inversion of reflectance spectra. On the one hand, we can relate a reflectance spectrum to a set of different forest structures. On the other hand, we could also attribute a reflectance spectrum to different leaf parameters [66].

These types of studies could also be conducted for different climate scenarios, for different management strategies and regions/biomes (e.g. using the large set of available forest parameterizations for FORMIND [64,67]). Lookup tables and artificial intelligence can help us analyze such large sets of forests and their reflectance spectra and, if desired, even offer the possibility to incorporate additional information about the forests using the forest model.

5. Conclusions

In this work we have applied an adapted version of the radiative transfer model mScope to a complex vegetation structure modelled by the individual-based forest model FORMIND. We showed that weighted averaging of leaf parameters could be a useful approach to simulate reflectance of forests with different species mixtures (simple/detailed representation). The investigated types of forest representation provide good simulated reflectance spectra (for optical and NIR - range) compared to satellite measurements. However, which type of forest representation provides the best results is influenced by forest structure. In respect to vegetation indices the best results were obtained assuming the simple or detailed forest representation. Good correlations were found between simulated and measured vegetation indices (especially NDVI). For future studies, we intend to take advantage of the detailed representation of forest, and plan to study more heterogeneous forest stands, such as tropical forests. In combination with the forest model, many new perspectives emerge that provide the opportunity to better understand the relationship between forest reflectance and forest properties.

Author Contributions: Conceptualization, H.H., F.J.B. and A.H.; methodology, H.H.; software, H.H., K.S. and A.H.; formal analysis, H.H.; data curation, H.H. and K.S.; writing—original draft preparation, H.H. and A.H. ; writing—review and editing, H.H., F.J.B. and A.H.; visualization, H.H.; supervision, F.J.B. and A.H.; project administration, A.H.. All authors have read agreed to the published version of the manuscript.

Funding: The research was supported with funding from the Helmholtz Research Program "Changing Earth - Sustaining our Future" / Topic 5 "Future Landscapes" (POF-IV, 2021-2027).

Institutional Review Board Statement: Not applicable.

Informed Consent Statement: Not applicable.

Data Availability Statement: The code of the forest model FORMIND is available at formind.org. The code of the radiative transfer model mScope is available at github.com/peiqiyang/mSCOPE. All leaf parameters used in this study are available through the CABO data portal data.caboscience. org/leaf.

Acknowledgments: We thank Javier Pacheco-Labrador for providing help regarding the code of mScope.

Conflicts of Interest: The authors declare no conflict of interest. The funders had no role in the design of the study; in the collection, analyses, or interpretation of data; in the writing of the manuscript; or in the decision to publish the results.

Abbreviations

 The following abbreviations are used in this manuscript:

RTM	Radiative Transfer Model
mScope	multilayer Soil Canopy Observation of Photochemistry and Energy fluxes
LAI	Leaf Area Index
SWIR	Short Wave Infrared
NIRS	Near Infrared Spectrum
RMSE	Root Mean Square Error
MAE	Mean Absolute Error
NDVI	Normalized Difference Vegetation Index
EVI	Enhanced Vegetation Index
MSI	Moisture Stress Index
NDMI	Normalized Difference Moisture Index
kNDVI	kernel NDVI
SAD	Spectral Angle Distance

Appendix A. Additional information on the method section

Figure A1. Study map of the 28 forest stands in the region North Karelia (blue area), Finland. The forest stands are distributed over an area of 150 km × 150 km.
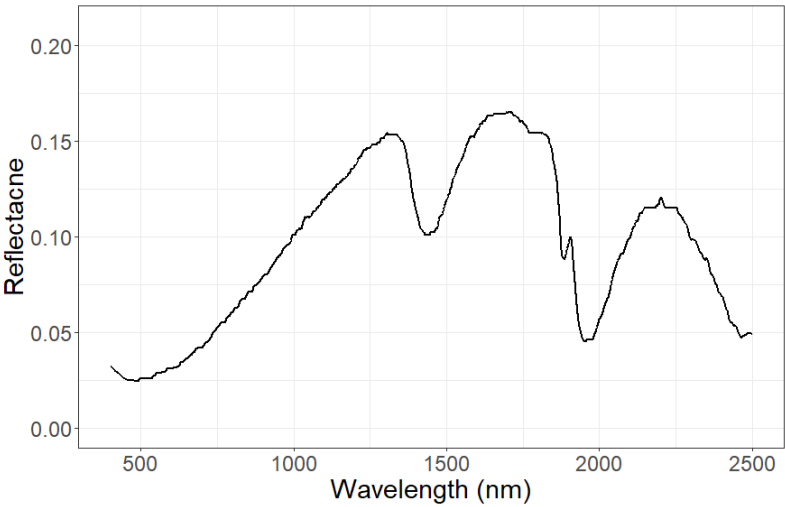
Figure A2. Soil reflection. Shown is assumed the reflection of wet soil. We assume for all forest stands the same soil reflectance.

<div align="center">

Table A1. Leaf parameters

</div>

Leaf parameter	Picea Abies	Pinus Silvestrys	Betula (Pendula and Pubescens)
Cab $[\mu\mathrm{g\ cm}^{-2}]$	21.94	23.92	36.71
Cdm $[\mathrm{g\ cm}^{-2}]$	0.024	0.025	0.006
Cw [cm]	0.03	0.03	0.0117
Cs $[-]$	0.01	0.01	0.01
Car $[\mu\mathrm{g\ cm}^{-2}]$	4.40	4.50	8.62
N $[-]$	1.25	1.24	1.77

Table A2. Attributes of the forest stands from Finland used for this study (28 plots, 30 m × 30 m).

plot number [−]	basal area [m²ha⁻¹]	maximum height [m]	height heterogeneity [m]	species richness [−]	species evenness [−]	biomass [t_odm ha⁻¹]	LAI [−]
1	28.78	30.09	5.31	3	0.49	148.30	3.93
2	19.63	28.63	3.47	2	0.35	106.83	3.23
3	16.31	26.38	2.88	2	0.26	90.74	2.69
4	22.25	29.21	4.54	2	0.41	118.74	3.46
5	19.87	29.71	4.64	5	0.74	109.47	2.26
6	32.84	30.80	4.04	2	0.04	170.06	4.84
7	17.60	23.84	3.36	4	0.16	94.34	3.13
8	17.33	24.59	2.37	3	0.17	95.09	2.94
9	25.66	26.10	3.69	5	0.25	133.24	2.39
10	27.03	30.01	4.59	2	0.05	139.91	3.98
11	17.02	22.70	2.92	3	0.27	85.02	3.15
12	27.35	23.32	3.39	3	0.65	114.86	4.07
13	20.38	21.67	3.28	3	0.59	88.96	2.64
14	18.37	23.34	2.77	1	0.00	86.37	1.67
15	21.37	26.22	3.38	3	0.44	105.38	2.37
16	27.37	26.44	4.08	3	0.10	139.98	2.52
17	24.54	28.80	4.52	2	0.38	125.61	2.58
18	30.99	28.45	4.24	2	0.07	152.92	4.71
19	30.12	28.74	3.61	3	0.47	162.74	3.56
20	30.42	30.30	3.92	2	0.35	164.55	4.52
21	17.60	23.34	2.45	2	0.06	84.49	1.60
22	27.16	25.85	3.96	2	0.43	120.19	3.54
23	29.31	27.40	4.08	2	0.16	139.35	4.44
24	25.45	21.70	2.63	3	0.38	89.55	5.04
25	30.72	27.96	4.61	3	0.62	145.02	4.58
26	26.66	34.41	5.57	4	0.69	138.13	3.67
27	22.03	22.77	2.95	3	0.55	95.38	2.64
28	22.10	25.73	3.21	3	0.50	114.78	2.97

Basal area is defined by the cross-sectional area of trees at breast height. Maximum height describes the highest tree height in the forest stand. Height heterogeneity describes the standard deviation of tree height. Richness describes the number of species in the forest. Evenness is defined by the normalized Shannon index. Biomass describes the sum of all tree biomass.

Table A3. Spectral configuration of the 10 Sentinel-2A bands used in this study [28].

spectral band	center wavelength [nm]	band name	band width [nm]	spatial resolution [m]
B02	490	blue	65	10
B03	560	green	35	10
B04	665	red	30	10
B05	705	red-edge 1	15	20
B06	740	red-edge 2	15	20
B07	783	red-edge 3	20	20
B08	842	NIR 1	115	10
B08a	865	NIR 2	20	20
B11	1610	SWIR 1	90	20
B12	2190	SWIR 2	180	20
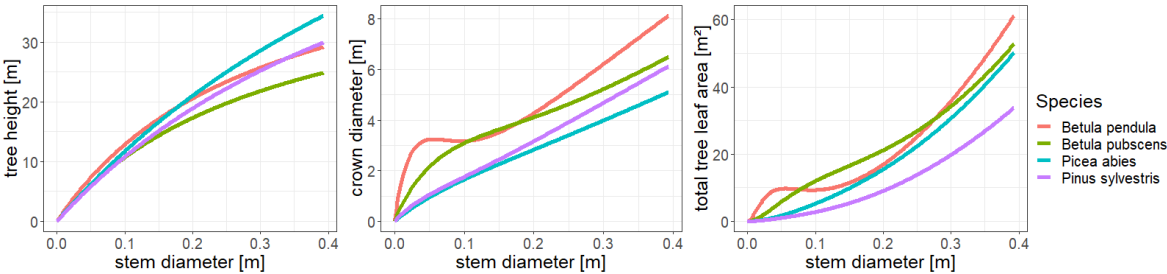
Figure A3. Analysis of allometries in FORMIND. Shown are the relationships between stem diameter and tree height, crown diameter as well as the total leaf area of a tree for the tree species simulated in FORMIND.
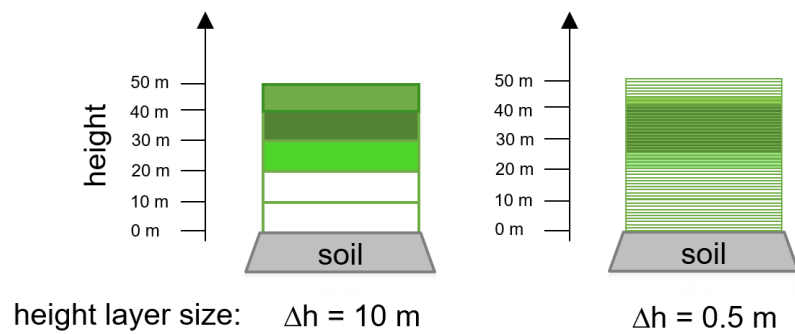
Figure A4. Concept of height layers. Shown is the same forest with a different resolution of height layers (Δh = 10 m and Δh = 0.5 m). Each layer includes different species mixtures (indicated by colour). We use 5 height layers in the case Δh = 10 m and 100 height layers in the case Δh = 0.5 m. All layers which contain leaves contributes to the resulting reflectance spectrum. Empty height layers (no leaves are in the layer) do not influence the reflectance spectrum (details see section 2.4).
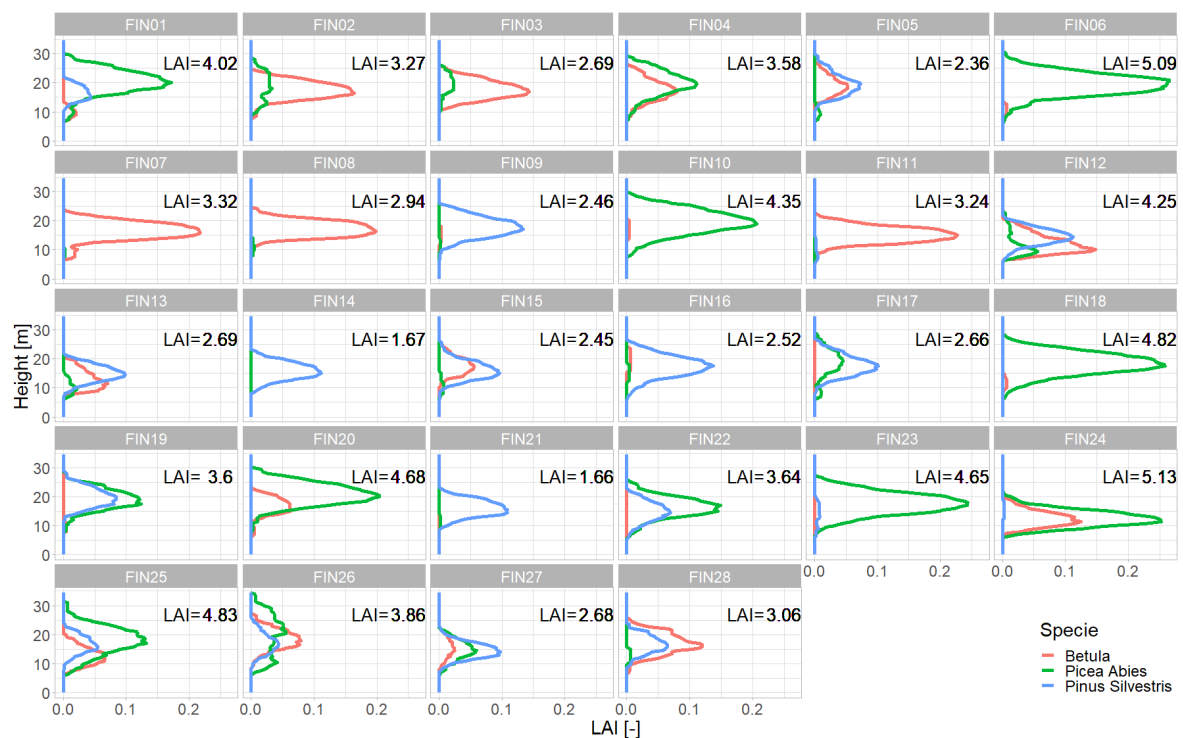
Figure A5. LAI Profiles for each forest stand. Shown are the LAI values (x-axis) in each height layer (y-axis) per species (red – Betula, green – Picea Abies, blue - Pinus Sylvestris). The colored lines show the LAI for a particular species (sum of all trees of the species in the plot). So, the sum of all the lines gives the LAI profile of all trees in the plot.

Appendix B. Additional information on the result section
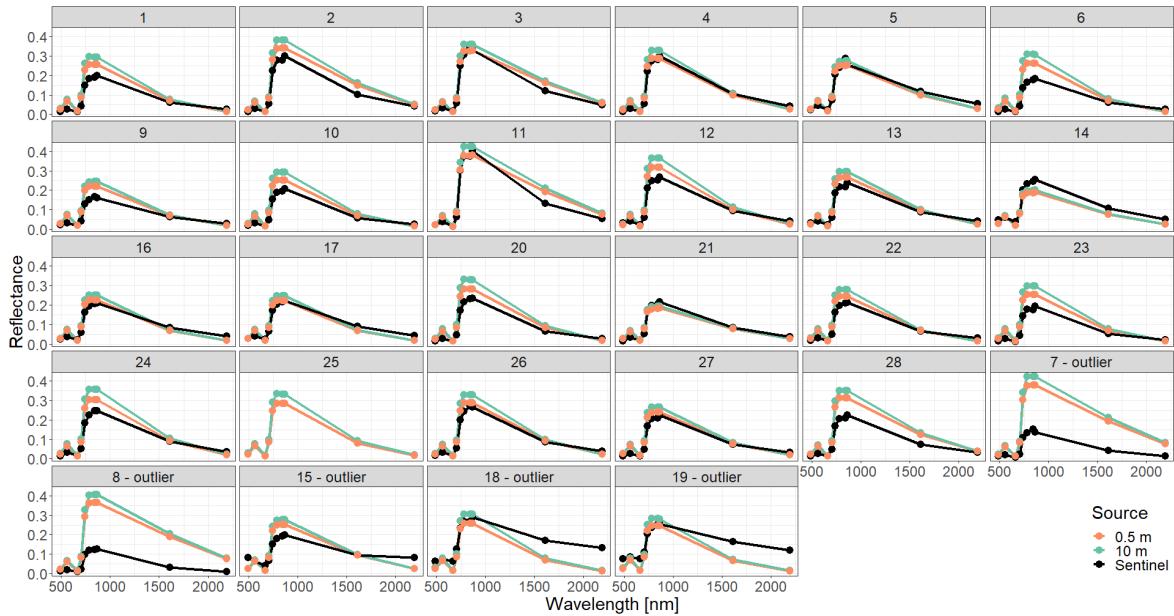
Figure A6. Comparison of simulated reflectance spectra with Sentinel measurements assuming a simple forest representation using different descriptions of the vertical forest structure (0.5 m or 10 m height layers). The Sentinel 2 spectrum of plot 25 is not provided by [28].
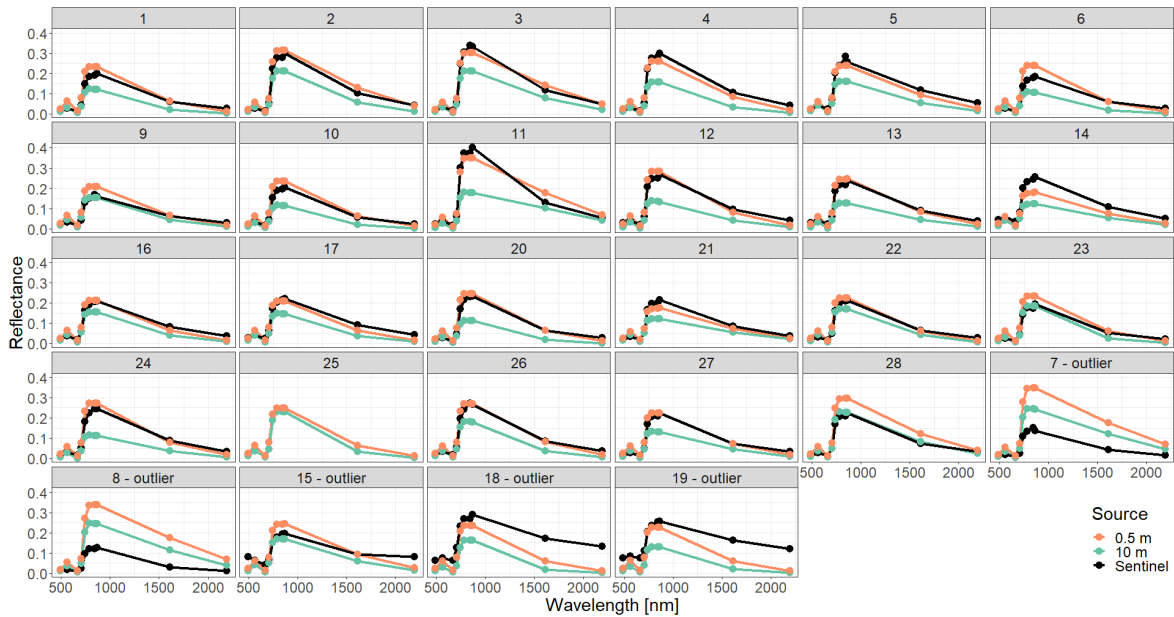
Figure A7. Comparison of simulated reflectance spectra with Sentinel measurements assuming a detailed forest representation using different descriptions of the vertical forest structure (0.5 m or 10 m height layers).
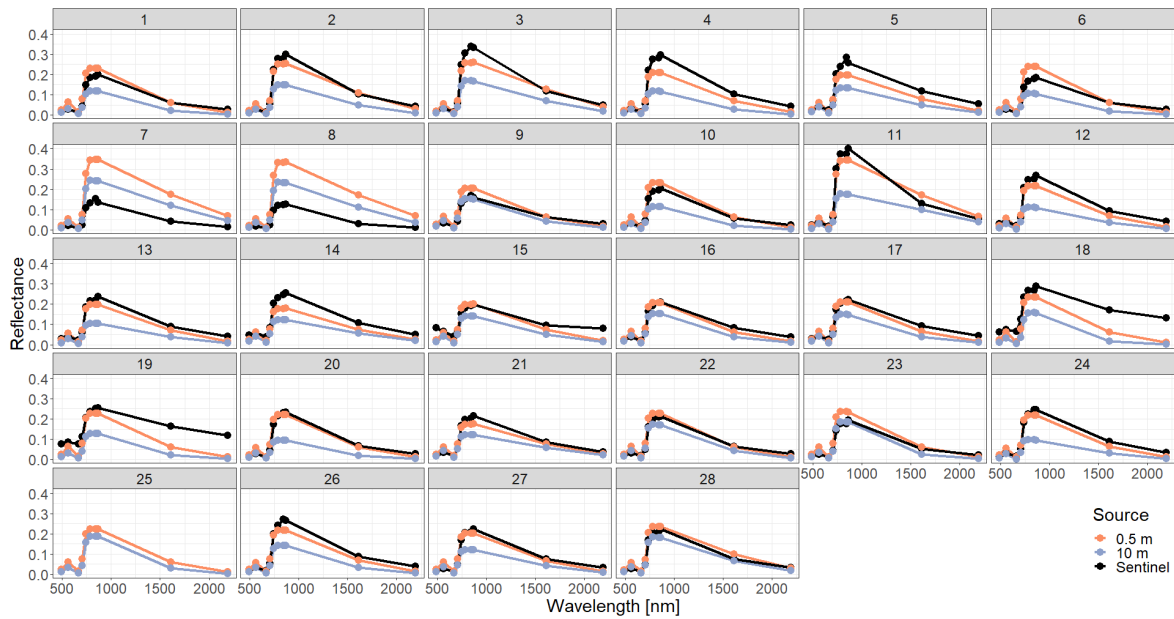
Figure A8. Comparison of simulated reflectance spectra with Sentinel measurements assuming a spectra-averaged forest representation using different descriptions of the vertical forest structure (0.5 m or 10 m height layers).
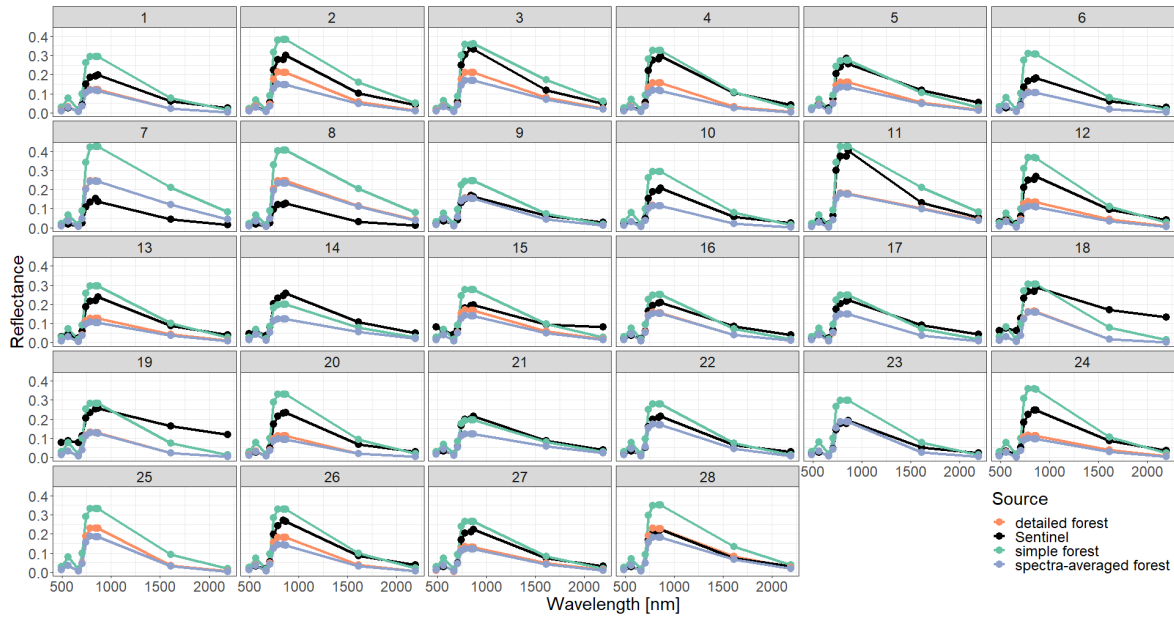
Figure A9. Comparison of simulated reflectance spectra with Sentinel measurements assuming different types of forest representations (simple, detailed and specta-averaged) and using 10 m height layers for the description of vertical forest structure.
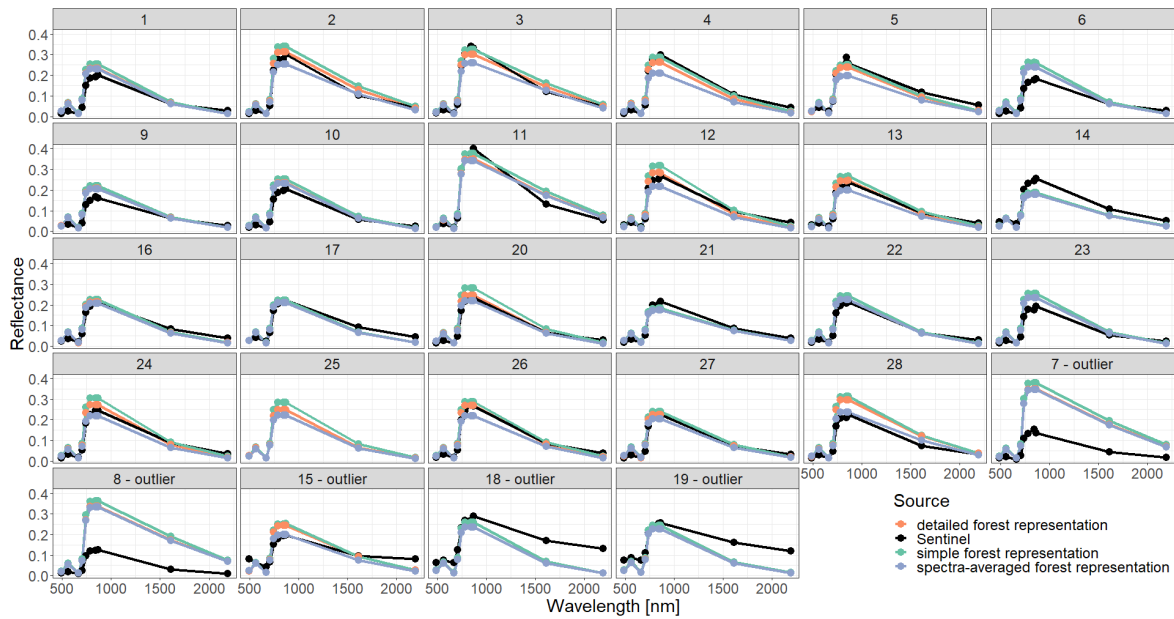
Figure A10. Comparison of simulated reflectance spectra with Sentinel measurements assuming different types of forest representations (simple, detailed, spectra averaged) and using 0.5 m height layers for the description of vertical forest structure.
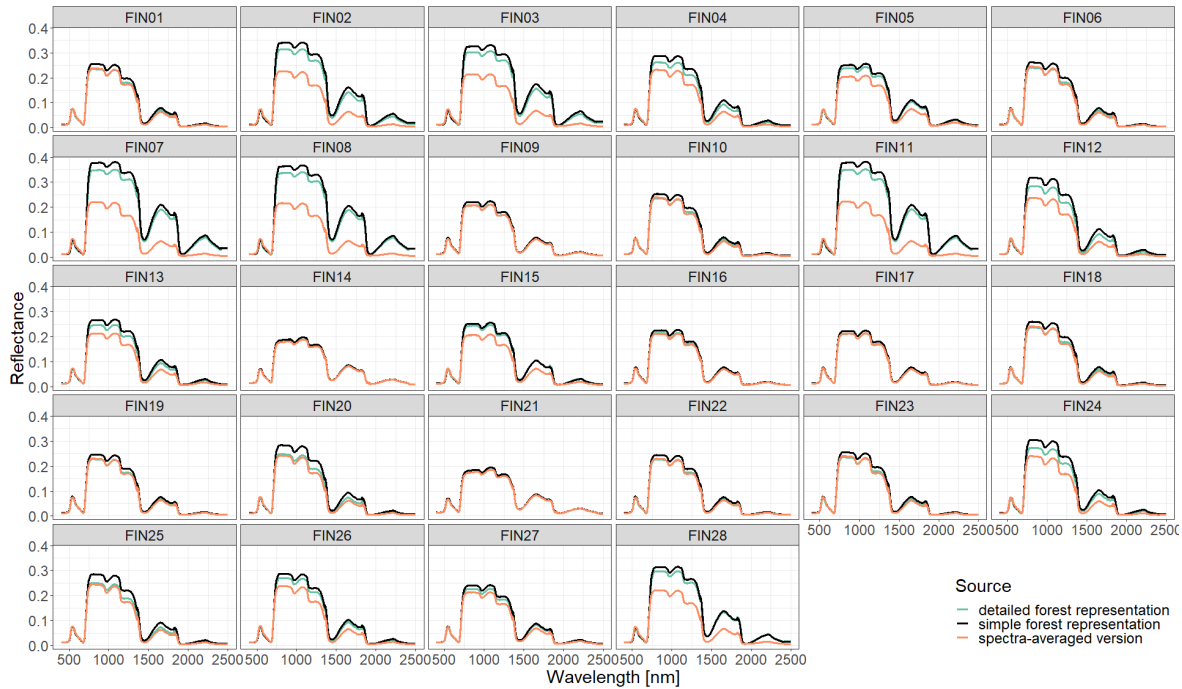
Figure A11. Comparison of simulated reflectance spectra assuming different types of forest representations (simple, detailed, spectra averaged) and using 0.5 m height layers for the description of vertical forest structure. The resolution of the simulated reflectance wavelengths is 1 nm.
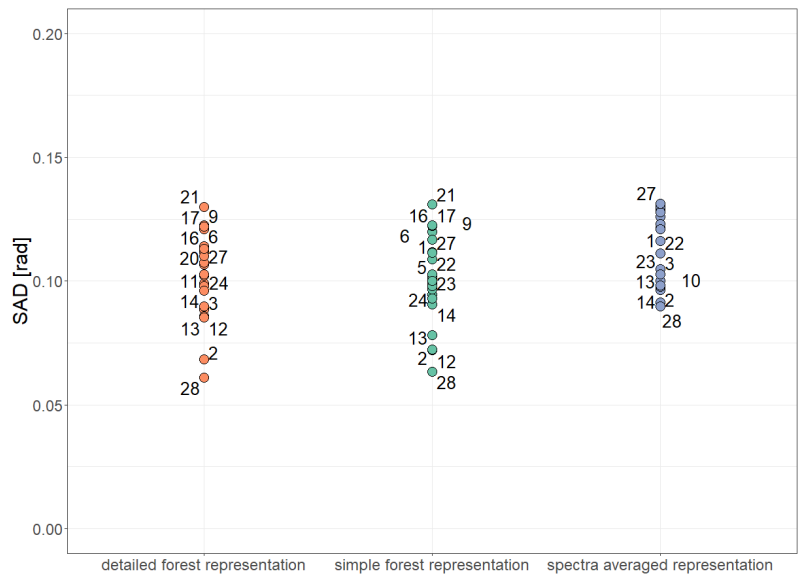
Figure A12. Comparison of simulated reflectance spectra and measured reflectance spectra using a distance index (Spectral Angle Distance, 0 rad: identical, $\frac{\pi}{2}$ rad: different). Results are shown for 28 forest plots (dots) and different forest representations. Comparison has been done for 10 wavebands of Sentinel-2.
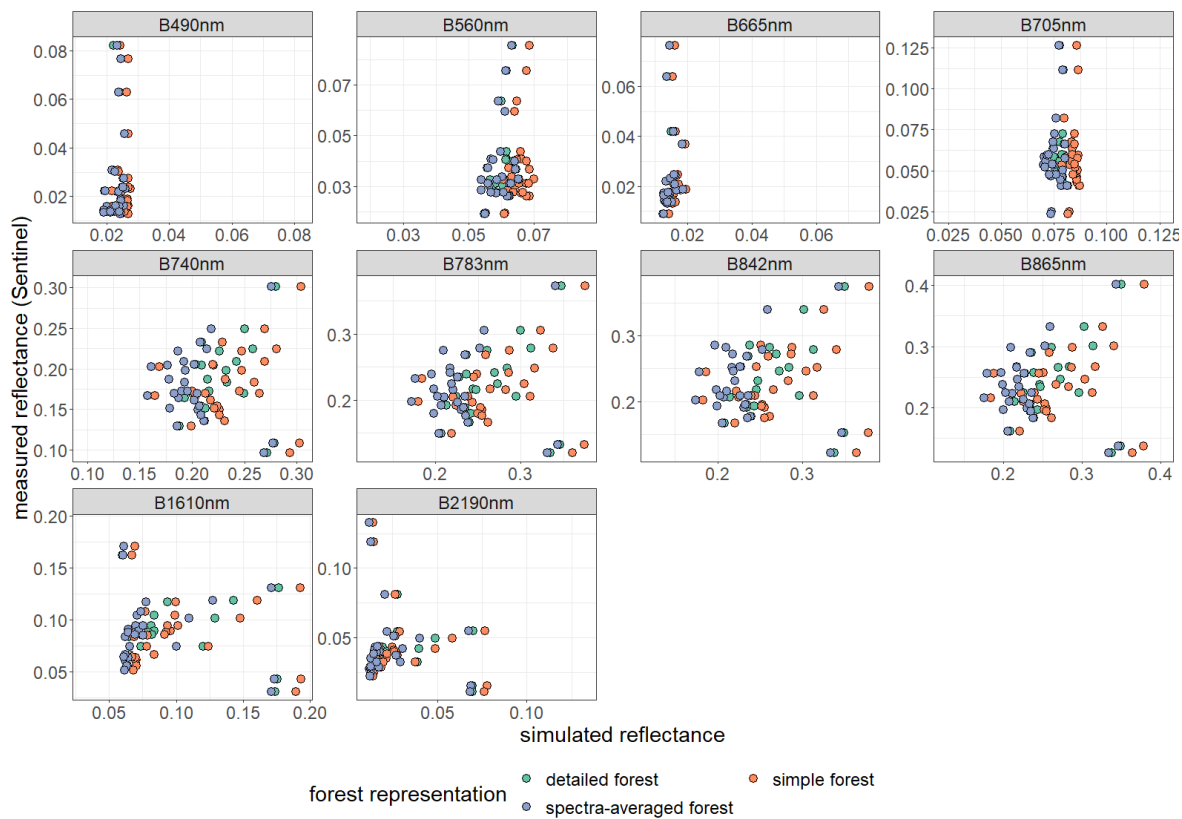
Figure A13. Comparison of simulated and measured reflectance of 28 forest stands (dots) and different forest representations (indicated by colors). Please note, the scales used for the illustration of measured and simulated reflectance differs for each band. Reflectance has been averaged for 10 wavebands (described by centred wavelengths, for more information on wavebands see Table A3).

Appendix C. Analysis of selected forest stands (outliers)
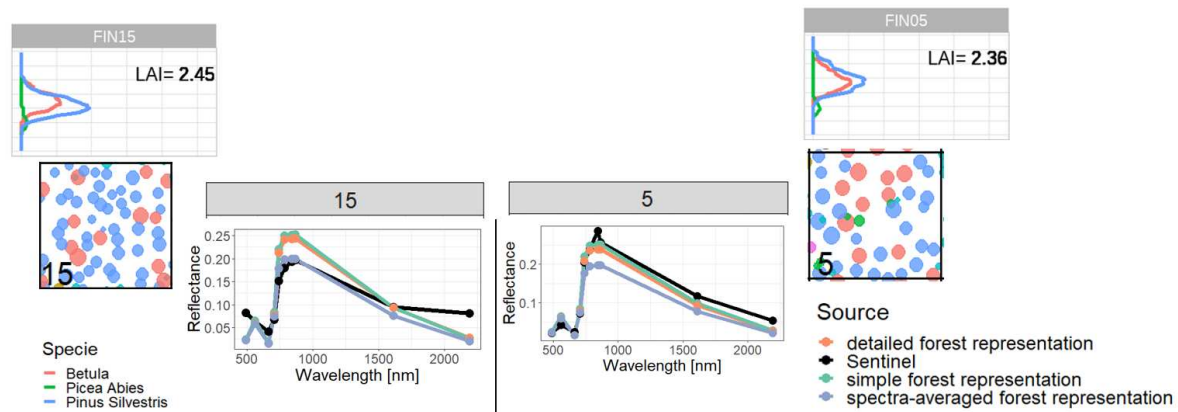
Figure A14. Comparison of reflectance spectra and additional information of forest stand 15 (classified as outlier) with forest stand 5. We compare forest properties of an outlier (left side) with forest properties of a forest with similar attributes, which is not an outlier (right side). Therefore, we compare the LAI profile (outer sides top), the reflectance spectra (in the middle) and the species composition (outer sides bottom). Despite the similar LAI distribution and species composition we got different Sentinel-measurements for reflectance, but similar simulated reflectance.
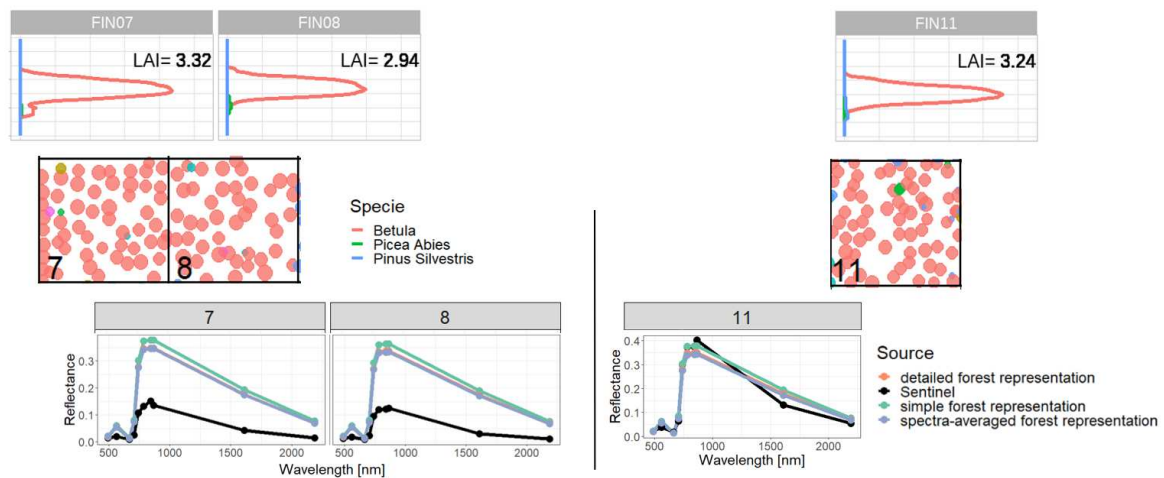
Figure A15. Comparison of reflectance spectra and additional information of forest stands 7 and 8 (classified as outliers) with forest stand 11. We compare forest properties of two outliers (left side) with forest properties of a forest with similar attributes, which is not an outlier (right side). Therefore, we compare the LAI profile (outer sides top), the reflectance spectra (in the middle) and the species composition (outer sides bottom). Despite the similar LAI distribution and species composition we got different Sentinel-measurements for reflectance, but similar simulated reflectance.
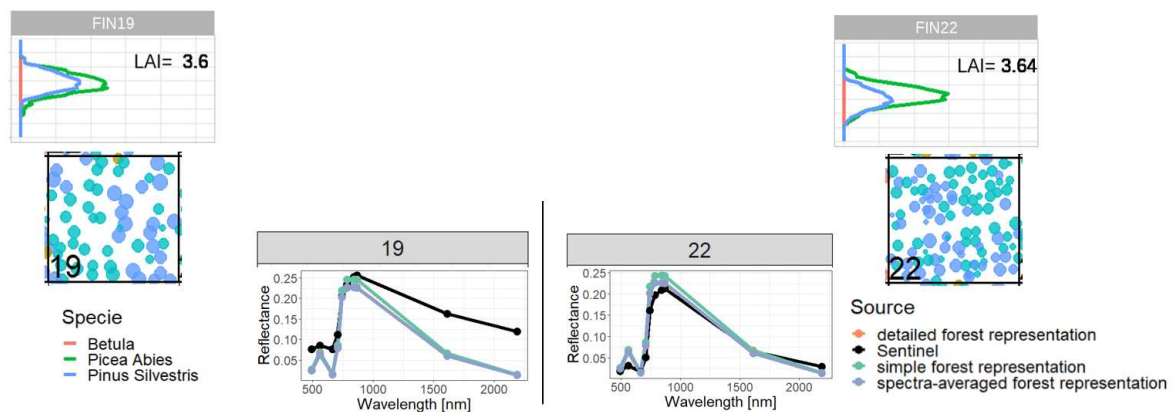
Figure A16. Comparison of reflectance spectra and additional information of forest stand 19 (classified as outlier) with forest stand 22. We compare forest properties of an outlier (left side) with forest properties of a forest with similar attributes, which is not an outlier (right side). Therefore, we compare the LAI profile (outer sides top), the reflectance spectra (in the middle) and the species composition (outer sides bottom). Despite the similar LAI distribution and species composition we got different Sentinel-measurements for reflectance, but similar simulated reflectance.
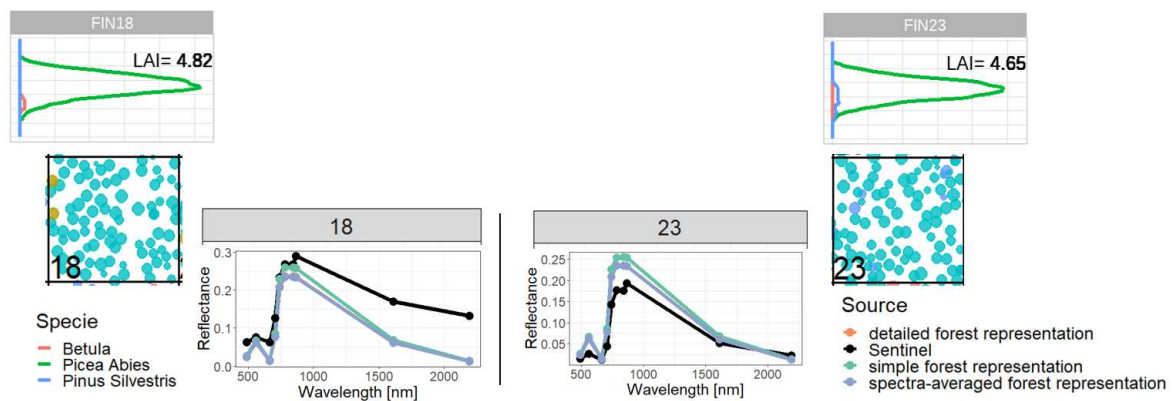
Figure A17. Comparison of reflectance spectra and additional information of forest stand 18 (classified as outlier) with forest stand 23. We compare forest properties of an outlier (left side) with forest properties of a forest with similar attributes, which is not an outlier (right side). Therefore, we compare the LAI profile (outer sides top), the reflectance spectra (in the middle) and the species composition (outer sides bottom). Despite the similar LAI distribution and species composition we got different Sentinel-measurements for reflectance, but similar simulated reflectance.

Appendix D. Analysis of LAI and additional indices
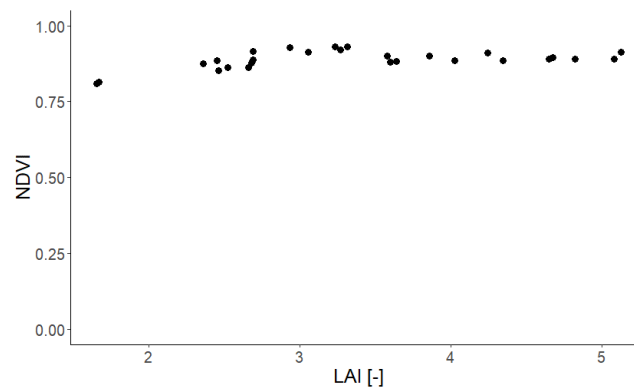
Figure A18. Relationship between LAI (x-axis, field data) and NDVI (y-axis, Sentinel-2 measurements) of 28 Finland forest stands.
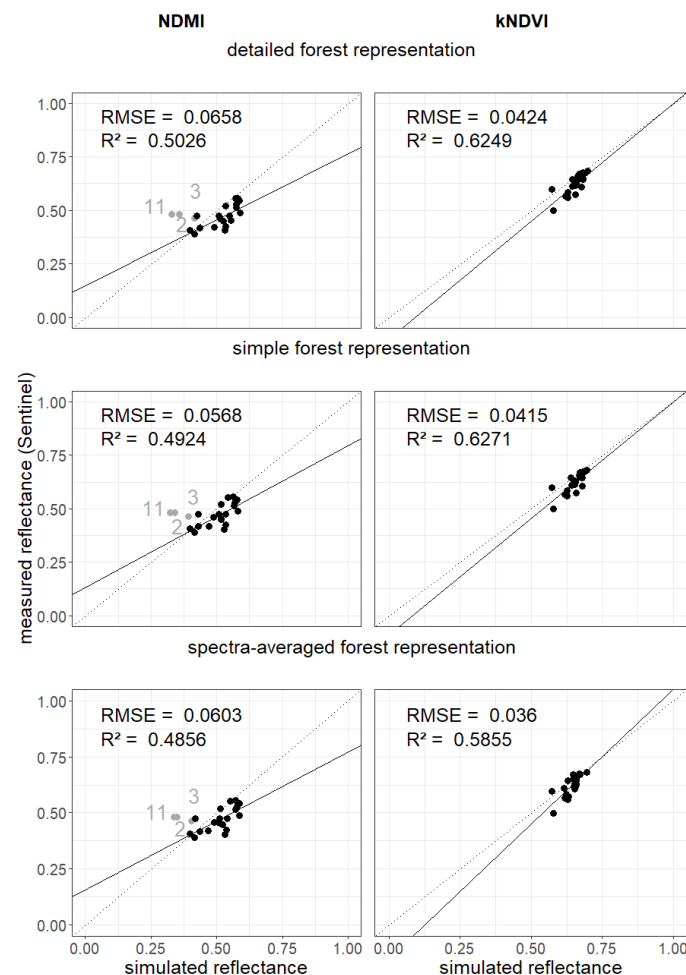
Figure A19. Comparison of vegetation indices for 28 forest stands in Finland. The vegetation indices (NDMI left, kNDVI right) for the measured reflectance spectra in the different wavebands for the simulated reflectance spectra (x-axis) and for the satellite measurements (y-axis). In each row, a different forest representation is is assumed (1. detailed forest representation, 2. simple forest representation, 3. spectra-averaged forest representation; more information about the cases in section 2.3). Each point represents a forest stand in Finland (gray points indicate outliers that are not used to calculate the RMSE and R^2 - see Appendix Figure A14 – A17).

Table A4. Analysis of vegetation indices for different forest representations. The mean Spectral Angle Distance is calculated as average of the SAD of 28 forest stands for each forest representation (height layer size = 0.5 m). More details about the vegetation indices and Spectral Angle Distance can be found in Section 2.4, Fig. 5 and Fig. A19.

	simple forest	detailed forest	spectra averaged forest
NDVI			
R^2	0.63	0.63	0.59
bias R^2	−0.086	−0.097	−0.177
RMSE	0.04	0.04	0.033
MAE	0.033	0.034	0.027
EVI			
R^2	0.43	0.45	0.25
bias R^2	0.086	0.059	0.116
RMSE	0.107	0.081	0.074
MAE	0.092	0.069	0.062
MSI			
R^2	0.49	0.49	0.47
bias R^2	0.141	0.162	0.164
RMSE	0.051	0.059	0.054
MAE	0.041	0.05	0.043
NDMI			
R^2	0.49	0.5	0.49
bias R^2	0.133	0.15	0.156
RMSE	0.057	0.066	0.060
MAE	0.046	0.056	0.049
kNDVI			
R^2	0.63	0.62	0.59
bias R^2	−0.089	−0.098	−0.15
RMSE	0.041	0.042	0.036
MAE	0.034	0.035	0.029
mean SAD	0.101	0.103	0.113

References

1. Pan, Y.; Birdsey, R.A.; Fang, J.; Houghton, R.; Kauppi, P.E.; Kurz, W.A.; Phillips, O.L.; Shvidenko, A.; Lewis, S.L.; Canadell, J.G.; et al. A Large and Persistent Carbon Sink in the World's Forests. *Science* **2011**, *333*, 988–993. https://doi.org/10.1126/science.1201609.
2. Malhi, Y. The carbon balance of tropical forest regions, 1990–2005. *Current Opinion in Environmental Sustainability* **2010**, *2*, 237–244. https://doi.org/10.1016/j.cosust.2010.08.002.
3. Ciais, P.; Sabine, C.L.; Bala, G.; Bopp, L.; Brovkin, V.A.; Canadell, J.G.; Chhabra, A.; DeFries, R.S.; Galloway, J.N.; Heimann, M.; et al., Carbon and Other Biogeochemical Cycles. In *Climate Change 2013 – The Physical Science Basis: Working Group I Contribution to the Fifth Assessment Report of the Intergovernmental Panel on Climate Change*; Cambridge University Press, 2014; pp. 465—-570. https://doi.org/10.1017/CBO9781107415324.015.
4. FAO. The State of the World's Forests 2022. Forest pathways for green recovery and building inclusive, resilient and sustainable economies. **2022**. https://doi.org/10.4060/cb9360en.
5. Gibson, L.; Lee, T.M.; Koh, L.P.; Brook, B.W.; Gardner, T.A.; Barlow, J.; Peres, C.A.; Bradshaw, C.J.; Laurance, W.F.; Lovejoy, T.E.; et al. Primary forests are irreplaceable for sustaining tropical biodiversity. *Nature* **2011**, *478*, 378–381.
6. Myers, N.; Mittermeier, R.A.; Mittermeier, C.G.; Da Fonseca, G.A.; Kent, J. Biodiversity hotspots for conservation priorities. *Nature* **2000**, *403*, 853–858.
7. Pimm, S.L.; Jenkins, C.N.; Abell, R.; Brooks, T.M.; Gittleman, J.L.; Joppa, L.N.; Raven, P.H.; Roberts, C.M.; Sexton, J.O. The biodiversity of species and their rates of extinction, distribution, and protection. *science* **2014**, *344*, 1246752.

8.   Pan, Y.; Birdsey, R.A.; Phillips, O.L.; Jackson, R.B. The structure, distribution, and biomass of the world's forests. *Annual Review of Ecology, Evolution, and Systematics* **2013**, *44*, 593–622.

9.   Guanter, L.; Kaufmann, H.; Segl, K.; Foerster, S.; Rogass, C.; Chabrillat, S.; Kuester, T.; Hollstein, A.; Rossner, G.; Chlebek, C.; et al. The EnMAP spaceborne imaging spectroscopy mission for earth observation. *Remote Sensing* **2015**, *7*, 8830–8857.

10. Moorcroft, P.R.; Hurtt, G.C.; Pacala, S.W. A method for scaling vegetation dynamics: the ecosystem demography model (ED). *Ecological monographs* **2001**, *71*, 557–586.

11. Lawrence, D.M.; Oleson, K.W.; Flanner, M.G.; Thornton, P.E.; Swenson, S.C.; Lawrence, P.J.; Zeng, X.; Yang, Z.L.; Levis, S.; Sakaguchi, K.; et al. Parameterization improvements and functional and structural advances in version 4 of the Community Land Model. *Journal of Advances in Modeling Earth Systems* **2011**, *3*.

12. Maréchaux, I.; Langerwisch, F.; Huth, A.; Bugmann, H.; Morin, X.; Reyer, C.P.; Seidl, R.; Collalti, A.; Dantas de Paula, M.; Fischer, R.; et al. Tackling unresolved questions in forest ecology: The past and future role of simulation models. *Ecology and Evolution* **2021**, *11*, 3746–3770. https://doi.org/10.1002/ece3.7391.

13. Shugart, H.H.; Wang, B.; Fischer, R.; Ma, J.; Fang, J.; Yan, X.; Huth, A.; Armstrong, A.H. Gap models and their individual-based relatives in the assessment of the consequences of global change. *Environmental Research Letters* **2018**, *13*, 033001.

14. Köhler, P.; Huth, A. The effects of tree species grouping in tropical rainforest modelling: Simulations with the individual-based model Formind. *Ecological Modelling* **1998**, *109*, 301–321. https://doi.org/10.1016/S0304-3800(98)00066-0.

15. Smith, B. LPJ-GUESS-an ecosystem modelling framework. *Department of Physical Geography and Ecosystems Analysis, INES, Sölvegatan* **2001**, *12*, 22362.

16. Sellers, P.J. Canopy reflectance, photosynthesis and transpiration. *International journal of remote sensing* **1985**, *6*, 1335–1372.

17. Kokhanovsky, A.A.; Kuusk, A.; Lang, M.; Kuusk, J. Database of optical and structural data for the validation of forest radiative transfer models. *Light Scattering Reviews 7: Radiative Transfer and Optical Properties of Atmosphere and Underlying Surface* **2013**, pp. 109–148.

18. Kuusk, A. Canopy Radiative Transfer Modeling. In *Comprehensive Remote Sensing*; Liang, S., Ed.; Elsevier: Oxford, 2018; pp. 9–22. https://doi.org/10.1016/B978-0-12-409548-9.10534-2.

19. Brazhnik, K.; Shugart, H. Model sensitivity to spatial resolution and explicit light representation for simulation of boreal forests in complex terrain. *Ecological Modelling* **2017**, *352*, 90–107.

20. Deutschmann, T.; Beirle, S.; Frieß, U.; Grzegorski, M.; Kern, C.; Kritten, L.; Platt, U.; Prados-Román, C.; Puķīte, J.; Wagner, T.; et al. The Monte Carlo atmospheric radiative transfer model McArtim: Introduction and validation of Jacobians and 3D features. *Journal of Quantitative Spectroscopy and Radiative Transfer* **2011**, *112*, 1119–1137.

21. Verhoef, W.; Jia, L.; Xiao, Q.; Su, Z. Unified optical-thermal four-stream radiative transfer theory for homogeneous vegetation canopies. *IEEE Transactions on geoscience and remote sensing* **2007**, *45*, 1808–1822.

22. Bonan, G.B.; Lawrence, P.J.; Oleson, K.W.; Levis, S.; Jung, M.; Reichstein, M.; Lawrence, D.M.; Swenson, S.C. Improving canopy processes in the Community Land Model version 4 (CLM4) using global flux fields empirically inferred from FLUXNET data. *Journal of Geophysical Research: Biogeosciences* **2011**, *116*.

23. Medvigy, D.; Wofsy, S.; Munger, J.; Hollinger, D.; Moorcroft, P. Mechanistic scaling of ecosystem function and dynamics in space and time: Ecosystem Demography model version 2. *Journal of Geophysical Research: Biogeosciences* **2009**, *114*.

24. Bonan, G.; Williams, M.; Fisher, R.; Oleson, K. Modeling stomatal conductance in the earth system: linking leaf water-use efficiency and water transport along the soil–plant–atmosphere continuum. *Geoscientific Model Development* **2014**, *7*, 2193–2222.

25. Gastellu-Etchegorry, J.P.; Lauret, N.; Yin, T.; Landier, L.; Kallel, A.; Malenovský, Z.; Bitar, A.A.; Aval, J.; Benhmida, S.; Qi, J.; et al. DART: Recent Advances in Remote Sensing Data Modeling With Atmosphere, Polarization, and Chlorophyll Fluorescence. *IEEE Journal of Selected Topics in Applied Earth Observations and Remote Sensing* **2017**, *10*, 2640–2649. https://doi.org/10.1109/JSTARS.2017.2685528.

26. Yang, P.; Verhoef, W.; van der Tol, C. The mSCOPE model: A simple adaption to the SCOPE model to describe reflectance, fluorescence and photosynthesis of vertically heterogeneous canopies. *Remote Control of Environment* **2017**, *201*, 1–11. https://doi.org/10.1016/j.rse.2017.08.029.

27. Baeten, L.; Verheyen, K.; Wirth, C.; Bruelheide, H.; Bussotti, F.; Finér, L.; Jaroszewicz, B.; Selvi, F.; Valladares, F.; Allan, E.; et al. A novel comparative research platform designed to determine the functional significance of tree species diversity in European forests. *Perspectives in Plant Ecology, Evolution and Systematics* **2013**, *15*, 281–291. https://doi.org/10.1016/j.ppees.2013.07.002.

28. Ma, X.; Mahecha, M.D.; Migliavacca, M.; van der Plas, F.; Benavides, R.; Ratcliffe, S.; Kattge, J.; Richter, R.; Musavi, T.; Baeten, L.; et al. Inferring plant functional diversity from space: the potential of Sentinel-2. *Remote Sensing of Environment* **2019**, *233*, 111368. https://doi.org/10.1016/j.rse.2019.111368.

29. Paulick, S.; Dislich, C.; Homeier, J.; Fischer, R.; Huth, A. The carbon fluxes in different successional stages: modelling the dynamics of tropical montane forests in South Ecuador. *Forest Ecosystems* **2017**, *4*, 1–11.

30. Rödig, E.; Cuntz, M.; Rammig, A.; Fischer, R.; Taubert, F.; Huth, A. The importance of forest structure for carbon fluxes of the Amazon rainforest. *Environmental Research Letters* **2018**, *13*, 054013.

31. Köhler, P.; Huth, A. Simulating growth dynamics in a South-East Asian rainforest threatened by recruitment shortage and tree harvesting. *Climatic Change* **2004**, *67*, 95–117.

32. Gutiérrez, A.G.; Huth, A. Successional stages of primary temperate rainforests of Chiloé Island, Chile. *Perspectives in Plant Ecology, Evolution and Systematics* **2012**, *14*, 243–256.

33. Huth, A.; Ditzer, T. Long-term impacts of logging in a tropical rain forest—a simulation study. *Forest Ecology and management* **2001**, *142*, 33–51.

34. Kammesheidt, L.; Köhler, P.; Huth, A. Sustainable timber harvesting in Venezuela: a modelling approach. *Journal of applied ecology* **2001**, *38*, 756–770.

35. Köhler, P.; Chave, J.; Riéra, B.; Huth, A. Simulating the long-term response of tropical wet forests to fragmentation. *Ecosystems* **2003**, *6*, 0114–0128.

36. Köhler, P.; Huth, A. Impacts of recruitment limitation and canopy disturbance on tropical tree species richness. *ecological modelling* **2007**, *203*, 511–517.

37. Rüger, N.; Williams-Linera, G.; Kissling, W.D.; Huth, A. Long-term impacts of fuelwood extraction on a tropical montane cloud forest. *Ecosystems* **2008**, *11*, 868–881.

38. Fischer, R.; Armstrong, A.; Shugart, H.H.; Huth, A. Simulating the impacts of reduced rainfall on carbon stocks and net ecosystem exchange in a tropical forest. *Environmental modelling & software* **2014**, *52*, 200–206.

39. Bohn, F.J.; Frank, K.; Huth, A. Of climate and its resulting tree growth: Simulating the productivity of temperate forests. *Ecological Modelling* **2014**, *278*, 9–17. https://doi.org/10.1016/j.ecolmodel.2014.01.021.

40. Bruening, J.M.; Fischer, R.; Bohn, F.J.; Armston, J.; Armstrong, A.H.; Knapp, N.; Tang, H.; Huth, A.; Dubayah, R. Challenges to aboveground biomass prediction from waveform lidar. *Environmental Research Letters* **2021**, *16*, 125013.

41. Rüger, N.; Gutiérrez, A.G.; Kissling, W.D.; Armesto, J.J.; Huth, A. Ecological impacts of different harvesting scenarios for temperate evergreen rain forest in southern Chile—a simulation experiment. *Forest Ecology and Management* **2007**, *252*, 52–66.

42. Taubert, F.; Frank, K.; Huth, A. A review of grassland models in the biofuel context. *Ecological Modelling* **2012**, *245*, 84–93.

43. Reyer, C.P.O.; Silveyra Gonzalez, R.; Dolos, K.; Hartig, F.; Hauf, Y.; Noack, M.; Lasch-Born, P.; Rötzer, T.; Pretzsch, H.; Meesenburg, H.; et al. The PROFOUND Database for evaluating vegetation models and simulating climate impacts on European forests. *Earth System Science Data* **2020**, *12*, 1295–1320. https://doi.org/10.5194/essd-12-1295-2020.

44. van der Tol, C.; Verhoef, W.; Timmermans, J.; Verhoef, A.; Su, Z. An integrated model of soil-canopy spectral radiances, photosynthesis, fluorescence, temperature and energy balance. *Biogeosciences* **2009**, *6*, 3109–3129. https://doi.org/10.5194/bg-6-3109-2009.

45. Vilfan, N.; van der Tol, C.; Muller, O.; Rascher, U.; Verhoef, W. Fluspect-B: A model for leaf fluorescence, reflectance and transmittance spectra. *Remote Sensing of Environment* **2016**, *186*, 596–615. https://doi.org/10.1016/j.rse.2016.09.017.

46. Féret, J.B.; Gitelson, A.; Noble, S.; Jacquemoud, S. PROSPECT-D: Towards modeling leaf optical properties through a complete lifecycle. *Remote Sensing of Environment* **2017**, *193*, 204–215.

47. Verhoef, W. Light scattering by leaf layers with application to canopy reflectance modeling: The SAIL model. *Remote Sensing of Environment* **1984**, *16*, 125–141. https://doi.org/10.1016/0034-4257(84)90057-9.

48. Kothari, S.; Beauchamp-Rioux, R.; Blanchard, F.; Crofts, A.L.; Girard, A.; Guilbeault-Mayers, X.; Hacker, P.W.; Pardo, J.; Schweiger, A.K.; Demers-Thibeault, S.; et al. Predicting leaf traits across functional groups using reflectance spectroscopy. *New Phytologist* **2023**, *238*, 549–566.

49. Huete, A.; Didan, K.; Miura, T.; Rodriguez, E.P.; Gao, X.; Ferreira, L.G. Overview of the radiometric and biophysical performance of the MODIS vegetation indices. *Remote sensing of environment* **2002**, *83*, 195–213.

50. Gao, X.; Huete, A.R.; Ni, W.; Miura, T. Optical–biophysical relationships of vegetation spectra without background contamination. *Remote sensing of environment* **2000**, *74*, 609–620.

51. Camps-Valls, G.; Campos-Taberner, M.; Álvaro Moreno-Martínez.; Walther, S.; Duveiller, G.; Cescatti, A.; Mahecha, M.D.; Muñoz-Marí, J.; García-Haro, F.J.; Guanter, L.; et al. A unified vegetation index for quantifying the terrestrial biosphere. *Science Advances* **2021**, *7*, eabc7447. https://doi.org/10.1126/sciadv.abc7447.

52. Hardisky, M.H.; Klemas, V.; Smart, R. The influence of soil salinity, growth form, and leaf moisture on the spectral radiance of Spartina alterniflora Canopies. *Photogramm. Eng. Remote Sens* **1983**, *49*, 77–83.

53. Hunt Jr, E.R.; Rock, B.N. Detection of changes in leaf water content using near-and middle-infrared reflectances. *Remote sensing of environment* **1989**, *30*, 43–54.

54. Vogelmann, J.; Rock, B. Assessing forest decline in coniferous forests of Vermont using NS-001 Thematic Mapper Simulator data. *International Journal of Remote Sensing* **1986**, *7*, 1303–1321.

55. Kruse, F.A.; Lefkoff, A.; Boardman, J.; Heidebrecht, K.; Shapiro, A.; Barloon, P.; Goetz, A. The spectral image processing system (SIPS)—interactive visualization and analysis of imaging spectrometer data. *Remote sensing of environment* **1993**, *44*, 145–163.

56. Huete, A.R.; Liu, H.; Batchily, K.; van Leeuwen, W. A comparison of vegetation indices over a global set of TM images for EOS-MODIS. *Remote Sensing of Environment* **1997**, *59*, 440–451. https://doi.org/10.1016/S0034-4257(96)00112-5.

57. Bussotti, F.; Pollastrini, M. Evaluation of leaf features in forest trees: Methods, techniques, obtainable information and limits. *Ecological indicators* **2015**, *52*, 219–230.

58. Jacquemoud, S.; Ustin, S. *Leaf optical properties*; Cambridge University Press, 2019.

59. Kattenborn, T.; Fassnacht, F.E.; Schmidtlein, S. Differentiating plant functional types using reflectance: which traits make the difference? *Remote Sensing in Ecology and Conservation* **2019**, *5*, 5–19.

60. Kattenborn, T.; Richter, R.; Guimarães-Steinicke, C.; Feilhauer, H.; Wirth, C. AngleCam: Predicting the temporal variation of leaf angle distributions from image series with deep learning. *Methods in Ecology and Evolution* **2022**, *13*, 2531–2545.

61. Jacquemoud, S.; Verhoef, W.; Baret, F.; Bacour, C.; Zarco-Tejada, P.J.; Asner, G.P.; François, C.; Ustin, S.L. PROSPECT+ SAIL models: A review of use for vegetation characterization. *Remote sensing of environment* **2009**, *113*, S56–S66.

62. Verhoef, W.; Van Der Tol, C.; Middleton, E.M. Hyperspectral radiative transfer modeling to explore the combined retrieval of biophysical parameters and canopy fluorescence from FLEX–Sentinel-3 tandem mission multi-sensor data. *Remote sensing of environment* **2018**, *204*, 942–963.

63. Rödig, E.; Knapp, N.; Fischer, R.; Bohn, F.J.; Dubayah, R.; Tang, H.; Huth, A. From small-scale forest structure to Amazon-wide carbon estimates. *Nature communications* **2019**, *10*, 5088.

64. Henniger, H.; Huth, A.; Frank, K.; Bohn, F. Creating virtual forest around the globe: Forest Factory 2.0 and analysing the state space of forests. *Ecological Modelling* **2023**. https://doi.org/inpress.

65. Bohn, F.J.; Huth, A. The importance of forest structure to biodiversity–productivity relationships. *Royal Society open science* **2017**, *4*, 160521.

66. Pacheco-Labrador, J.; Perez-Priego, O.; El-Madany, T.S.; Julitta, T.; Rossini, M.; Guan, J.; Moreno, G.; Carvalhais, N.; Martín, M.P.; Gonzalez-Cascon, R.; et al. Multiple-constraint inversion of SCOPE. Evaluating the potential of GPP and SIF for the retrieval of plant functional traits. *Remote Sensing of Environment* **2019**, *234*, 111362.

67. Fischer, R.; Bohn, F.; Dantas de Paula, M.; Dislich, C.; Groeneveld, J.; Gutiérrez, A.G.; Kazmierczak, M.; Knapp, N.; Lehmann, S.; Paulick, S.; et al. Lessons learned from applying a forest gap model to understand ecosystem and carbon dynamics of complex tropical forests. *Ecological Modelling* **2016**, *326*, 124–133. https://doi.org/10.1016/j.ecolmodel.2015.11.018.